Environ Monit Assess (2010) 166:563–571
DOI 10.1007/s10661-009-1023-5

Monitoring aeolian desertification process in Hulunbir grassland during 1975–2006, Northern China

Guo Jian · Wang Tao · Xue Xian · Ma Shaoxiu · Peng Fei

Received: 31 August 2008 / Accepted: 3 June 2009 / Published online: 16 June 2009

Abstract The Hulunbir grassland experienced aeolian desertification expansion during 1975–2000, but local rehabilitation during 2000–2006. Northern China suffered severe aeolian desertification during the past 50 years. Hulunbir grassland, the best stockbreeding base in Northern China, was also affected by aeolian desertification. To evaluate the evolution and status of aeolian desertification, as well as its causes, satellite images (acquired in 1975, 1984, 2000, and 2006) and meteorological and socioeconomic data were interpreted and analyzed. The results show there was 2,345.7, 2,899.8, 4,053.9, and 3,859.6 km^2 of aeolian desertified land in 1975, 1984, 2000, and 2006, respectively. The spatial pattern dynamic had three stages: stability during 1975–1984, fast expansion during 1984–2000, and spatial transfer during 2000–2006. The dynamic degree of aeolian desertification is negatively related to its severity. Comprehensive analysis shows that the human factor is the primary cause of aeolian desertification in Hulunbir grassland. Although aeolian desertified land got partly rehabilitated, constant increase of extremely severe aeolian desertified land implied that current measures were not effective enough on aeolian desertification control. Alleviation of grassland pressure may be an effective method.

Keywords Aeolian desertification · Aeolian desertified land · Hulunbir grassland · Northern China · Aeolian desertification monitoring

J. Guo (✉) · T. Wang · X. Xue · S. Ma · F. Peng
Key Laboratory of Desert and Desertification, Institute of Cold and Arid Regions Environmental and Engineering Research, Chinese Academy of Sciences, No. 320 Donggang West Road, Lanzhou, 730000 Gansu Province, China
e-mail: keen@lzb.ac.cn

Introduction

Desertification, defined as "land degradation in arid, semiarid, and dry subhumid areas resulting from various factors, including climatic variations and human activities" (UNEP 1994), is a serious global environmental and ecological issue (Abubakar 1997; Warren 2002; Shen and Kheoruenromne 2003). More than 250 million people are directly affected by desertification worldwide. In addition, about one billion people in 110 countries are at risk of being affected by desertification (Ayoub 1999).

China is one of the countries mostly affected by desertification. In China, desertification has been divided into water erosion, salinization, and aeolian desertification (Wang and Zhu 2003). Specifically, aeolian desertification is defined as "land degradation in arid, semi-arid, and part of dry subhumid areas, characterized by former non-desert

area being replaced by desert-like landscape with sand drift activities, caused by excessive human activities under susceptible ecological conditions" (Zhu and Liu 1984). In northern China, aeolian desertification is the most common type, and it is distributed widely (Zhao et al. 2005). During the past 50 years, aeolian desertified land increased rapidly, with a ratio of 1,560 $km^2\ a^{-1}$ in the 1960s–1970s (Zhu et al. 1989), 2,100 $km^2\ a^{-1}$ in the 1980s (Zhu and Wang 1990), and 3,600 $km^2\ a^{-1}$ in the 1990s (Wang et al. 2003). Moreover, aeolian desertified land amounted to $38.57 \times 10^4\ km^2$, 15% of northern China's territory (Wang et al. 2004). The direct economic loss caused by desertification is about 54.1 billion Yuan a^{-1} (Zhang et al. 1996).

Hulunbir grassland is the most beautiful grassland and important stockbreeding base in China. Because of recent global warming and population growth, intense human activities, and irrational use of grassland, aeolian desertification is getting worse and worse (Nie et al. 2005). Recently, some researchers studied the status or dynamic change of aeolian desertification in Hulunbir grassland (Han and Zhang 1998; Feng and Wang 2004; Lv et al. 2005; Nie et al. 2005), but they lacked consecutive aeolian desertification monitoring and integrated cause analysis to explore the occurring mechanism of aeolian desertification. Besides this, spatial pattern changes and dynamic characteristics of aeolian desertification, especially the stability of aeolian desertified land with different severities, have not been reported in previous researches.

In this study, by means of remote sensing and geographic information system methods, the temporal and spatial evolution of aeolian desertification were reconstructed during 1975–2006 in Hulunbir grassland based on the establishment of a classification system for aeolian desertification in grassland (Table 1). Local natural environmental and socioeconomic data are analyzed to explore the mechanism and processes of aeolian desertification.

Study area

Hulunbir grassland in the northern China lies between 47°20′–50°15′ N latitude and 115°30′–121°10′ E longitude (Fig. 1). Administratively, the study area includes Hailar City, Manchuria City, Chenba'erhu Qi (a county is called Qi in Inner Mongolia), Xinba'erhuzuo Qi, Xinba'erhuyou Qi, and Ewenke Autonomous Qi, covering $8.36 \times 10^4\ km^2$. Hulunbir grassland has flat terrain, with elevation decreasing gradually from southeast to northwest, and with an average elevation of 600–800 m. Hulun Lake lies at the northeastern Xinba'erhuyou Qi, and several rivers, such as Hailar River, Wu'erxun River, Huihe River, and Yimin River, flow through the area. Sand, the material source of aeolian desertification, has

Table 1 Classification and indicators of aeolian desertification grades

Grades	Shifting sand (%)	Vegetation cover (%)	Land surface characteristics	Image features
L	< 5	> 60%	Blowout appears on windward slope of sand dunes and shifting sand is speckled	A sheet of light red, dotted by red
M	5%–25%	30%–60%	Shifting sand appears on windward slope of shrub sand dunes and flats between sand dunes	Irregular lark blocks and shape of sand dunes is clear
S	25%–50%	10%–30%	Sand dunes are in a half-shifting state, and shrubs withered widely	Irregular brownish yellow or yellow white mass, dotted shrubs can be identified
ES	> 50%	< 10%	Sand dunes in a shifting state, vegetation is very sparse	A big sheet of yellow white or incanus, shifting sand dunes or sand ridge can be identified

L land with light aeolian desertification, *M* land with moderate aeolian desertification, *S* land with severe aeolian desertification, *ES* land with extremely severe aeolian desertification

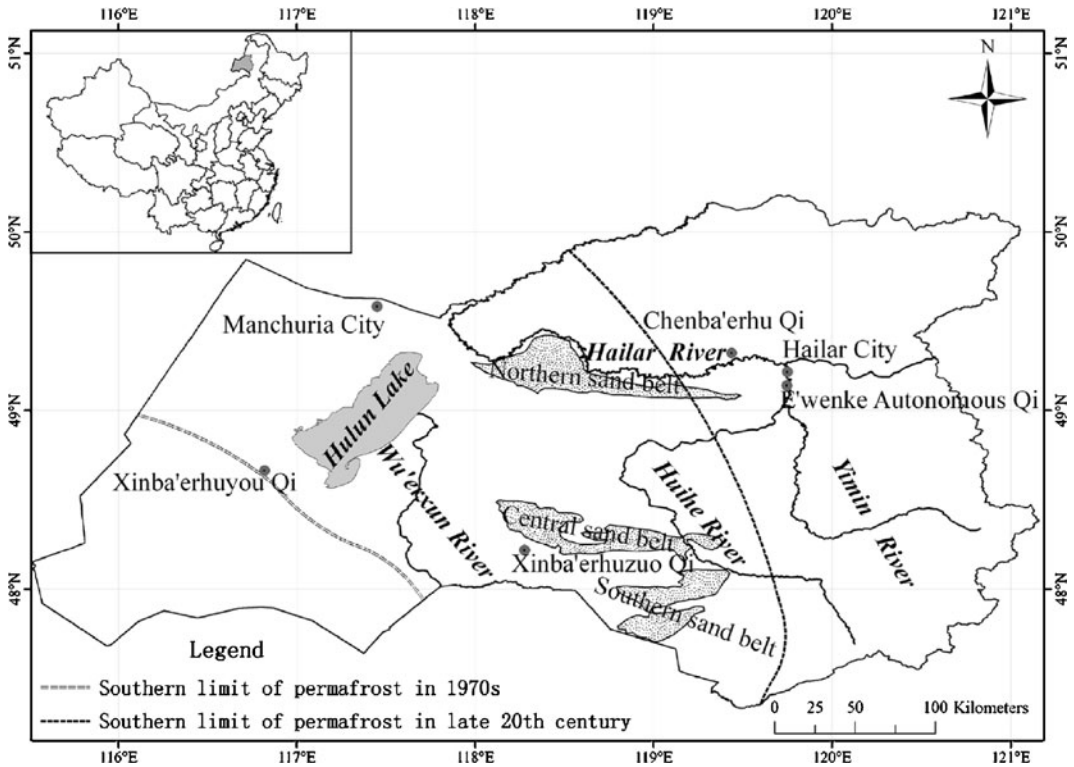

Fig. 1 Location of the study area

been transported into Hulunbir grassland by these rivers (Han and Zhang 1998). In the middle of Hulunbir grassland, there are three sand dune belts, commonly called the northern, central, and southern sand dune belts from north to south (Feng and Wang 2004), which are composed of fixed, semifixed, or shifting sand dunes (Fig. 1). The study area is controlled by semiarid and subhumid climates, characterized by dry and cold winters, arid and windy springs, and short summers. Annual air temperature is between −2.0°C and 0°C. Annual precipitation ranges from 235 to 380 mm, and 70% occurs during June–August. Annual evaporation is 1,100–1,630 mm, four to six times as much as precipitation. Annual mean wind velocity is 4.5 m/s, and average number of days with instantaneous wind velocity greater than 17.2 m/s is more than 30 days. Coincidence of windy weather and low vegetation cover in winter and spring and plenty of loose sand are the fundamental environmental conditions for aeolian desertification occurrence in Hulunbir grassland (Zhu et al. 1989).

Materials and methods

The dataset of more than 50 scenes of satellite images is used to monitor and map the process and spatial pattern of aeolian desertification in Hulunbir grassland, which include Landsat MSS images in 1975, Landsat 5 TM images in 1984, Landsant ETM in 2000, and Chinese Brazil Earth Resources Satellite (CBERS) images in 2006, and the spatial resolutions are 60 × 60, 30 × 30, 30 × 30, and 20 × 20 m, respectively. The Landsat images are obtained from Global Land Cover Facility (http://glcfapp.umiacs.umd.edu/), and CBERS data from the China Center for Resource Satellite Data and Applications (http://www.cresda.com.cn/). Images acquired in different seasons can influence the aeolian desertification monitoring

result greatly. According to previous researching results, autumn is the best season for aeolian desertification monitoring (Wu 2001a, b). So, of the images acquired in autumn, as many as possible were collected. Due to the influence of clouds, high-quality images are not available in some areas in autumn. In this case, clear images acquired in summer or spring will be chosen as replacements. Two scenes of images (P134R26 MSS in 1975 and P123R26 TM in 1984) are replaced by those acquired in spring and summer in the corresponding year.

False-color images obtained by stacking near infrared, red, and green bands and their geometrical correction were done by the Erdas Imagine 8.7 provided by ERDAS, and its accuracy was achieved within one pixel. The details of the satellite image processing were described by Navas and Machin (1997), Valle et al. (1998), and Vasconcelos et al. (2002). Evaluation of aeolian desertification includes not only the sum area of aeolian desertified land but also the degraded extent (Liu and Wang 2007). So, aeolian desertified land was classified into four grades: lightly, moderately, severely, and extremely severely aeolian desertified land, according to previous classification criteria shown in Table 1 (Wang et al. 2002, 2004). Field survey was carried out to relate image features to actual aeolian desertified land grades immediately after having acquired the CBERS images in autumn 2006. Aeolian desertified land grades were identified on the spot according to the classification criteria; meanwhile, locations were measured by global positioning system, and land surface features were also recorded by digital camera. As a result, image features corresponding to different grades of aeolian desertified land were summarized and listed in Table 1. All images were interpreted manually using ARCGIS 9.1, according to the criteria (Table 1). In order to confirm the reliability of interpreted results, a field survey was conducted again to resolve the questionable area in autumn 2007. At last, statistical data and spatial distribution maps of aeolian desertified land were obtained by ARCGIS 9.1 and were used to analyze the temporal changes and spatial pattern dynamics of aeolian desertification, and to reconstruct the development and evolution of aeolian desertification for the last 32 years. To detect the transfer among different grades of aeolian desertified land, the graphical superposition method introduced by Li et al. (2007) was employed to establish the aeolian desertified land transfer matrix. Meteorologic data from four stations (Hailar, Manchuria, Xinba'erhuzuo, and Xinba'erhuyou) and local annual population and amounts of livestock were also collected to analyze climatic variation and human activity changes, and their contribution to aeolian desertification in Hulunbir grassland.

Results and discussion

Dynamic change of aeolian desertification since 1975

Monitoring results (Table 2) show that aeolian desertified land kept expanding before 2000 and was gradually rehabilitated during 2000–2006 in Hulunbir grassland. In 1975, aeolian desertified land amounted to 2,345.7 km^2, and it increased to 2,899.8 km^2 with a rate of 61.6 km^2 a^{-1} in 1984. During 1984–2000, aeolian desertified land reached its largest area of 4,053.9 km^2, with the fastest increasing rate of 72.1 km^2 a^{-1} since 1975. After 2000, aeolian desertified land was rehabilitated, with a decreasing rate of 32.4 km^2 a^{-1}, and decreased to 3,859.7 km^2. It also indicates that lightly, moderately, and severely aeolian desertified land kept increasing before 2000, but decreased after 2000, except that extremely severe aeolian desertified land increased steadily all along since 1975.

Table 2 Dynamics of aeolian desertified land during the study period

Grades	Area/km^2			
	1975	1984	2000	2006
L	413.1	490.3	1,244.3	994.8
M	471.3	681.7	915.0	804.4
S	1,020.3	779.9	829.4	701.1
ES	441.0	947.9	1,065.2	1,359.4
Sum	2,345.7	2,899.8	4,053.9	3,859.6

L land with light aeolian desertification, *M* land with moderate aeolian desertification, *S* land with severe aeolian desertification, *ES* land with extremely severe aeolian desertification

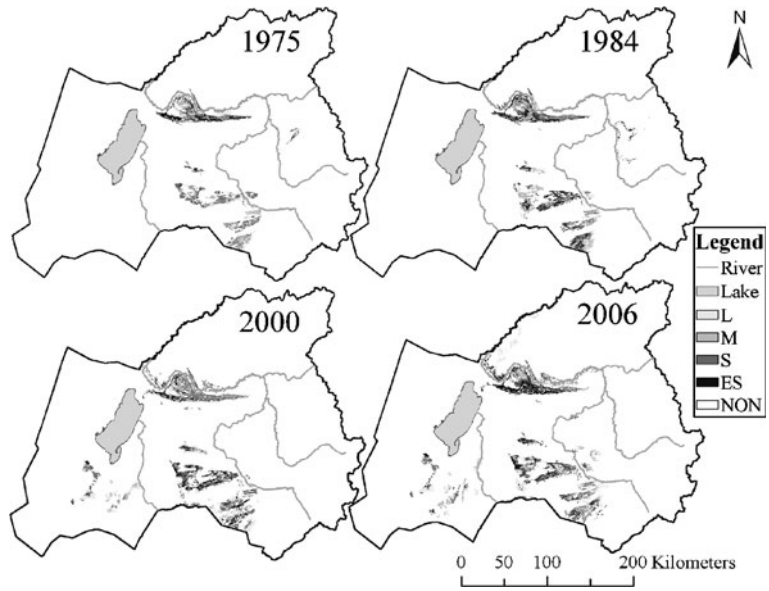

Fig. 2 Spatial distribution of various grades of aeolian desertified land in Hulunbir grassland at four stages

Spatial pattern change and transfer among different grades of aeolian desertified land

In 1975, aeolian desertified land was concentrated in the three sand dune belts (Figs. 1 and 2), and severely aeolian desertified land was the primary type, with an area of 1,020.3 km^2 and accounting for 43.5% of the sum area of aeolian desertified land. In 1984, aeolian desertified land did not expand too much spatially, but the extent of degradation was worsening. As shown in Table 3, from 1975 to 1984, there were 725.7 km^2

Table 3 Transfer matrix of different grades of aeolian desertified land

Transferred area (km^2)						
Year	Grades	L	M	S	ES	NON
1975–1984	L	179.0	53.6	48.6	33.6	98.4
	M	64.4	195.8	93.9	57.9	59.3
	S	73.8	176.3	486.5	275.1	8.6
	ES	24.5	36.5	64.6	310.0	5.4
	NON	148.6	219.5	86.3	271.3	80,543.7
Sum	Newly aeolian desertified: 725.7				Rehabilitated: 171.6	
1984–2000	L	208.8	136.4	46.0	29.8	69.2
	M	89.3	346.1	115.2	82.4	48.6
	S	62.9	77.0	495.7	125.0	19.4
	ES	44.2	75.6	80.9	739.4	7.8
	NON	839.1	279.9	91.5	88.5	79,416.1
Sum	Newly aeolian desertified: 1,299.1				Rehabilitated: 145.0	
2000–2006	L	794.9	62.4	25.8	27.7	333.5
	M	27.1	655.2	99.6	71.7	61.3
	S	20.0	20.2	493.2	273.9	22.1
	ES	11.0	13.1	58.1	970.6	12.5
	NON	141.9	53.5	24.4	15.4	79,326.0
Sum	Newly aeolian desertified: 235.2				Rehabilitated: 429.4	

L land with light aeolian desertification, *M* land with moderate aeolian desertification, *S* land with severe aeolian desertification, *ES* land with extremely severe aeolian desertification, *NON* nonaeolian desertified land

of nonaeolian desertified land becoming aeolian desertified land (newly aeolian desertified land), and 171.6 km^2 had turned into nonaeolian desertified land (rehabilitated). Meanwhile, 275.1 km^2 of severely aeolian desertified land has been further degraded to extremely severely sandy deserfied land; besides this, there is 148.6 km^2 of nonaeolian desertified land that actually consists of fixed sand dunes, transferred into extremely severely aeolian desertified land (Table 3). As a result, extremely severely aeolian desertified land had the largest area of 947.9 km^2 (Table 2), occupying 32.69% of the sum in 1984.

Compared to that in 1984, aeolian desertified land expanded widely in 2000. From 1984 to 2000, Fig. 2 shows clearly that much new aeolian desertified land appeared in flats between sand dunes, meadows around sand dune belts, reactivated sand dunes in the north of Hailar River, or meadows in the south of Hulunbir Lake. However, aeolian desertified land along Yimin River has been rehabilitated. According to Table 3, there is 1,299.1 km^2 of new aeolian desertified land, and 145.0 km^2 has been rehabilitated; among this, 839.1 km^2 is new lightly aeolian desertified land, contributing to 64.59% (Table 3). So, lightly aeolian desertified land amounted to 1,244.3 km^2 (Table 2) and became the largest portion, occupying 30.69%.

In 2006, much aeolian desertified land was rehabilitated around the southern sand dune belt and between sand dunes in the northern sand dune belt, while new aeolian desertified land appeared in the north of Hailar River and the east of Huihe River, mostly distributing along roads or around lakes (Fig. 2). During 2000–2006, 235.2 km^2 of nonaeolian desertified land was desertified and 429.4 km^2 was rehabilitated; therein, 333.5 km^2 of lightly aeolian desertified land was rehabilitated and 141.9 km^2 of nonaeolian desertified land was newly lightly aeolian desertified, accounting for 77.67% and 60.33% of the new desertification and rehabilitation, respectively (Table 3). Extremely severely aeolian desertified land kept increasing and reached its largest area of 1,359.4 km^2, occupying 35.22% of the sum area.

Characteristics of dynamic degree for different grades of aeolian desertified land

The dynamic degree is defined by the following function:

$$D_{(k)} = \mathrm{AT}_{(k)} \div \mathrm{AI}_{(k)} \times \frac{1}{t} \times 100\% \,, \tag{1}$$

where k is the grade of aeolian desertification, representing light, moderate, severe, or extremely severe aeolian desertification; $D_{(k)}$ is the dynamic degree of aeolian desertification of grade k; $\mathrm{AI}_{(k)}$ is the area of the kth grade of aeolian desertification in the initial year of a studying period; $\mathrm{AT}_{(k)}$ is the area of the kth grade of aeolian desertification, which has been transferred to other grades of aeolian desertification or nonaeolian desertification during the period; and t is the duration of the period. Dynamic degrees were computed for three periods, and the result is shown in Table 4. In general, the lighter the aeolian desertification grade is, the greater the dynamic degree is. However, the moderate grade had the greatest dynamic degree of 5.85% during 1975–1984, and the severe grade had the greatest value of 5.79% during 2000–2006. This was caused by the comparatively small area of moderately aeolian desertified land in 1975 (Table 2), and 273.9 km^2 of severely aeolian desertified land has been further degraded (Table 3). Noticeably, extremely severe aeolian desertification had the least dynamic degree for all the three periods, and the average value of 1.84% was less than half of the second least average value of 4.27% (Table 4). This suggests that extremely severely aeolian desertified land can hardly be rehabilitated.

Table 4 Dynamic degree of aeolian desertified land for different periods

Dynamic degree (%)				
Grades	1975–1984	1984–2000	2000–2006	Average
L	5.67	3.38	5.16	4.73
M	5.85	2.90	4.06	4.27
S	5.23	2.14	5.79	4.39
ES	2.97	1.29	1.27	1.84

Causes of aeolian desertification in Hulunbir grassland

Air temperature and precipitation trends

Climate is an important driving force for aeolian desertification (Zhu and Liu 1984). Air temperature and precipitation data recorded in four meteorological stations of Hailar, Manchuria, Xinba'erhuzuo, and Xinba'erhuyou were averaged to analyze the climate change trend in the study area. As is shown in Fig. 3, the annual average precipitation fluctuated violently, but without significant decreasing or increasing tendency during the past 46 years. Meanwhile, air temperature apparently increased more significantly during 1984–2000, with a ratio of 0.11°C a^{-1}. Increased air temperature can result in a more arid climate, which would favor the development of aeolian desertification.

Permafrost degradation

Permafrost can maintain soil moisture by preventing water from infiltrating or reducing evaporation, and it is also the water source for surface vegetation growth (Xue et al. 2007). Influenced by global warming and frequent human activities, permafrost degraded seriously in the last 100 years in northern China (Lu et al. 1993). Jin et al. (2006) mapped the shifting of the southern permafrost limit in China. The result is cited and shown in Fig. 1. From the early 1970s to the end of twentieth century, the southern permafrost limit shifted northward quickly (Fig. 1). Compared to Fig. 2, permafrost degraded exactly where aeolian desertified land was concentrated. Permafrost degradation can accelerate the aeolian desertification process by reducing soil moisture (Xue et al. 2007).

Human factors

Livestock amount and population increased by 3.9 and 6.6 times, respectively, from 1947 to 2006. There was no farmland before 1955, but it increased to 300 km^2 by 1,200 times during 1955–2006 (Fig. 4). It is noteworthy that aeolian desertification had a similar trend to human factors (Table 2, Fig. 4). In other words, aeolian desertification status was consistent with the change of human activities in Hulunbir grassland.

Before 1975, both livestock and farmlands fluctuated, and their trends were obscure; even though the population increased steadily, the population size was comparatively low (Fig. 4). It is suggested that human activity had a weak impact on aeolian desertification. Meanwhile, the aeolian desertified land had the lowest area during the

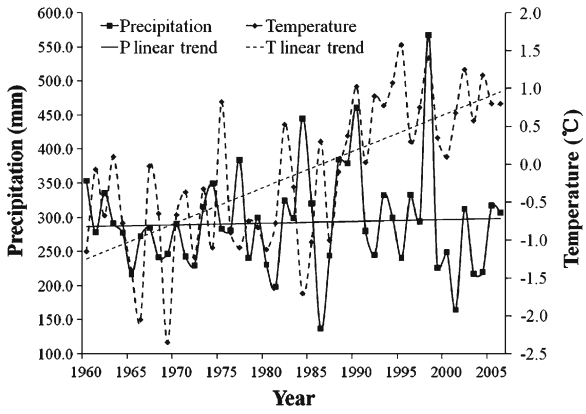

Fig. 3 Annual variation of precipitation and air temperature since 1960

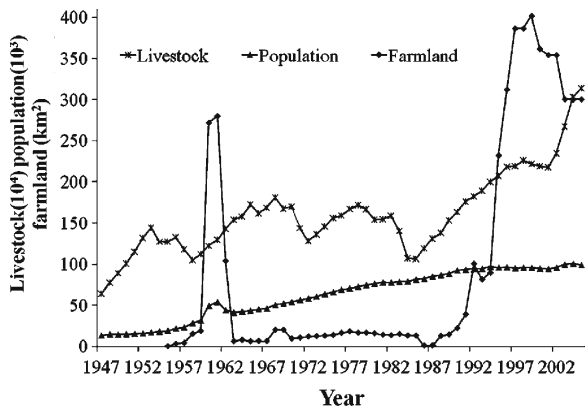

Fig. 4 Variation of population and livestock amount since 1947

study period, and its spatial range was limited in the three sand dune belts (Table 2, Fig. 2).

During 1975–1984, the population increased constantly, which resulted in more demands on firewood to get through the frigid winter and spring. Over-cutting led to the reactivation of a large area of fixed or semifixed sand dunes, which degraded to extremely severe sandy desertification (Table 3).

Human activity intensified greatly during 1984–2000, which was depicted by the sharp increase of livestock amount, population, and farmland (Fig. 4). Different from over-cutting, overgrazing cannot directly and rapidly result in serious aeolian desertification. In the beginning, it can only lead to vegetation degradation, characterized by decreased vegetation cover, disappearance of edible grass, and appearance of poisonous grass. If high pressure on the grassland continues, the land surface, with less protection of decreased vegetation cover and disruption by livestock, can suffer serious wind erosion on windy days. As a result, grassland is lightly aeolian desertified at first. If pressure is removed, lightly aeolian desertified land can recover by itself; otherwise, aeolian desertification will get more and more serious until the appearance of shifting sand dunes (Zhao et al. 2004). However, livestock can cause aeolian desertification in a wider range because of their mobility and great numbers (Zhu et al. 1989). Doubled livestock amount contributed much to the wide expansion of aeolian desertification during 1984–2000, which was exacerbated by coinstantaneous increase of the human population and rangeland reclamation.

In 2000, the Chinese Government launched the Conversion of Cropland to Forest or Grassland Program to protect arid or semiarid regions from aeolian desertification, which resulted in the decrease of farmland in Hulubir grassland (Fig. 4). Meanwhile, other measures were also taken to combat aeolian desertification. For example, aeolian desertified grassland was enclosed by fences and prohibited from being disturbed by livestock in order to allow it to rehabilitate naturally (Nie et al. 2005). Actually, this had a good effect on the rehabilitation of lightly aeolian desertified land, but it decreased the available grassland for livestock. In addition, livestock numbers have kept increasing since 2000 (Fig. 4). The healthy grassland has received more and more pressure beyond its carrying capacity, and it ultimately got aeolian desertified.

Conclusion

Aeolian desertified land kept expanding during 1975–2000, but it got locally rehabilitated after 2000. The spatial pattern dynamic had three stages: stability during 1975–1984, fast expansion during 1984–2000, and spatial transfer during 2000–2006. During the evolution of aeolian desertification, the dynamic degree is negatively related to the grade of aeolian desertification. Namely, the lighter the aeolian desertification grade is, the greater the dynamic degree is. Both natural and human factors contributed to the deterioration of aeolian desertification conditions before 2000, but consistent temporal and spatial variation of aeolian desertification and human activities indicated that anthropogenic factors should be the primary cause. Since 2000, the increase of air temperature and livestock promised continuous expansion of aeolian desertification, but some aeolian desertification control measures reversed this status. However, rehabilitation of aeolian desertified land is at the cost of the occurrence of aeolian desertification somewhere else. The result is more similar to aeolian desertified land being transferred somewhere else than to the land being rehabilitated. The basic reason is that land pressure has not lightened entirely but partly. In fact, land pressure was aggravated due to the constant increase of the population, especially livestock, during 2000–2006 (Fig. 4). So, current measures only have a temporary effect on aeolian desertification control, but they cannot promote the rehabilitation of aeolian desertification eventually. Alleviation of excessive human pressure on grassland could be an effective method.

Acknowledgements This research is supported by Innovation Project (No. O650445002) of the Chinese Academy of Sciences. We acknowledge the Global Land Cover Facility team and the China Center for Resource Satellite Data and Applications for their kind sharing of satellite images.

We also thank the China Meteorological Administration and Xinba'erhuzuo Qi Government for providing climate and socioeconomic data. Special appreciation is given to anonymous reviewers for their comments.

References

Abubakar, S. M. (1997). Monitoring land degradation in the semiarid tropics using an inferential approach: The Kabomo Basin case study, Nigeria. *Land Degradation & Development, 8*, 311–323. doi:10.1002/(SICI)1099-145X(199712)8:4<311::AID-LDR262>3.0.CO;2-8.

Ayoub, A. T. (1999). *Indicators of dryland degradation: Drylands, sustainable use of rangelands into the twenty-first century*. Rome: International Fund for Agricultural Development.

Feng, J. M., & Wang, T. (2004). Study on the actual and historical evolution of desertification in the Hulunbir Grassland. *Arid Land Geography, 27*(3), 356–360.

Han, G., & Zhang, G. F. (1998). The evolution characteristic of aeolian desertification in Hulunbuir Steppe during the past 30 years and its control strategies. *Journal of Desert Research, 18*(3), 221–225.

Jin, H. J., Li, S. X., & Cheng, G. D. (2006). Permafrost and climatic change in China. *Global and Planetary Change, 26*(4), 387–404. doi:10.1016/S0921-8181(00)00051-5.

Li, S., Zheng, Y., Luo, P., & Wang, X. (2007). Desertification in western Hainan Island, China (1959 to 2003). *Land Degradation & Development, 18*, 473–485. doi:10.1002/ldr.787.

Liu, S. L., & Wang, T. (2007). Aeolian desertification from the mid-1970s to 2005 in Otindag Sandy Land, Northern China. *Environmental Geology, 51*, 1057–1064. doi:10.1007/s00254-006-0375-1.

Lu, G. W., Weng, B. L., & Guo, D. X. (1993). The geographic boundary of permafrost in the northeast of China. *Journal of Glaciology and Geocryology, 15*(2), 214–218.

Lv, S. H., Lu, X. S., & Jin, W. L. (2005). Studies on wind erosion desertification and methods of reversion in Hulunbir Steppe. *Journal of Arid Land Resource Environment, 19*(3), 59–63.

Navas, A., & Machin, J. (1997). Assessing erosion risks in the gypsiferous steppe of Litigio (NE Spain). An approach using GIS. *Journal of Arid Environments, 37*, 433–441. doi:10.1006/jare.1997.0302.

Nie, H. G., Yue, L. P., & Yang, W. (2005). Present situation, evolution trend and causes of aeolian desertification in Hulunbuir Steppe. *Journal of Desert Research, 25*(5), 635–639.

Shen, R., & Kheoruenromne, I. (2003). Monitoring land use dynamics in Chanthaburi province of Thailand using digital remotely sensed images. *Pedosphere, 13*(2), 157–164.

UNEP (1994). *United Nations convention to combat desertification in those countries experiencing serious drought and/or desertification, particularly in Africa* (pp. 1–2). Geneva: United Nations Environment Programme for the Convention to Combat Desertification (CCD).

Valle, H. F., Elissalde, N. O., Gagliardini, D. A., & Milovich, J. (1998). Status of desertification in the Patagonian Region: Assessing and mapping from satellite imagery. *Arid Soil Research and Rehabilitation, 12*, 95–122.

Vasconcelos, M., Mussa Biai, J. C., Araujo, A., & Diniz, M. A. (2002). Land cover changes in two protected areas of Guinea-Bissau (1956–1998). *Applied Geography (Sevenoaks, England), 22*, 139–156. doi:10.1016/S0143-6228(02)00005-X.

Warren, A. (2002). Land degradation is contextual. *Land Degradation & Development, 13*, 449–459. doi:10.1002/ldr.532.

Wang, T., & Zhu, Z. D. (2003). Study on aeolian desertification in China—1. Definition of aeolian desertification and it's connotation. *Journal of Desert Research, 23*(3), 209–214.

Wang, T., Zhu, Z. D., & Wu, W. (2002). Aeolian desertification in the north China. *Science in China. Series D, 45*(Supp.), 23–34.

Wang, T., Wu, W., & Xue, X. (2003). Time-space evolution of desertification land in northern China. *Journal of Desert Research, 23*(3), 230–235.

Wang, T., Wu, W., & Xue, X. (2004). Spatial-temporal changes of aeolian desertified land during last 5 Decades in northern China. *Acta Geographica Sinica, 59*(2), 203–212.

Wu, W. (2001a). Using the TM image for monitoring land desertification. *Journal of Desert Research, 16*(2), 86–90.

Wu, W. (2001b). Study on desertification process in Mu Us sand land for last 50 years, China. *Journal of Desert Research, 21*(2), 164–169.

Xue, X., Guo, J., & Zhang, F. (2007). Development and cause of aeolian desertification in alpine region—in case of Maduo county in Yellow River source area. *Journal of Desert Research, 27*(5), 725–732.

Zhang, Y., Ning, D., & Smil, V. (1996). An estimate of economic loss for desertification in China. *China Population Resources and Environment, 6*, 45–49.

Zhao, H. L., Zhang, T. H., Zhao, X. Y., & Zhou, R. L. (2004). Effect of grazing on sandy grassland ecosystem in Inner Mongolia. *Chinese Journal of Applied Ecology, 15*(3), 420–424.

Zhao, H. L., Zhao, X. L., Zhou, R. L., Zhang, T. H., & Drakeb, S. (2005). Desertification processes due to heavy grazing in sandy rangeland, Inner Mongolia. *Journal of Arid Environments, 62*, 309–319. doi:10.1016/j.jaridenv.2004.11.009.

Zhu, Z. D., & Liu, S. (1984). The concept of aeolian desertification and the differentiation of its development. *Journal of Desert Research, 4*(3), 2–8.

Zhu, Z. D., & Wang, T. (1990). An analysis of the trend of land desertification in northern China during the last decade based on examples from some typical areas. *Acta Geographica Sinica, 45*(4), 430–440.

Zhu, Z. D., Liu, S., & Di, X. M. (1989). *Aeolian desertification and its control in China* (pp. 5–7). Beijing: Science.